

Two methods to control neutral-point voltage fluctuation for a hybrid VIENNA rectifier

Wei-Zhang Song^{1,2}, Nan Xie¹, You-Yun Wang², Zhi-Hao Dai¹, Wheeler Pat³

¹School of Automation and Information Engineering, Xi'an University of Technology, Xi'an, Shaanxi, People's Republic of China

²State Key Laboratory of Large Electric Drive System and Equipment Technology, Tianshui, Gansu, People's Republic of China

³School of Electrical and Electronic Engineering, University of Nottingham, Nottingham, UK
E-mail: songwz464237@126.com

Published in *The Journal of Engineering*; Received on 6th March 2018; Accepted on 6th March 2018

Abstract: This study presents two neutral-point balance control methods for a hybrid VIENNA rectifier, which is composed of a parallel system of a single-switch three-phase Boost rectifier and a VIENNA rectifier. Each rectifier in this topology processes part of the output power, therefore, a highly efficient and reliable performance is achieved in this rectifier system. However, the unbalance voltage of two DC-link capacitors in the VIENNA-type three level rectifier is also reflected in this hybrid rectifier. The fluctuation reason in neutral-point has been analysed using a mathematical model, meanwhile, the two methods with a hybrid algorithm and a simplified method based on zero-sequence component injection are proposed to control neutral-point fluctuation in this hybrid rectifier system. Furthermore, the performance comparison between these two methods is provided. The effectiveness of the two control methods has been verified using experimental results.

1 Introduction

The hybrid VIENNA rectifier is composed of a parallel system of a single switch three-phase Boost rectifier and a VIENNA-type three level rectifier. This hybrid rectifier has the following advantages:

It can achieve higher efficiency and reliable performance than the single rectifier [1–3].

The input current of the hybrid rectifier is divided into two parts, thus, the input power and current stress for the power switches in every single rectifier can be reduced [3–5].

The neutral-point voltage fluctuation is an inherent problem in three level topology including a hybrid VIENNA rectifier, which will cause the capacitors' voltage unbalanced and make the power device over voltage damage. Neutral-point voltage fluctuation will also affect the line voltage waveform in the same filter parameters, furthermore, the total harmonic distortion (THD) of input current becomes large [6]. Recently, some neutral-point suppression methods have been proposed. In [7], the neutral-point potential balance is controlled according to the operation time of P and N small vectors based on a three-level space vector modulation strategy, which is more complex and difficult to apply in control system. In [8], a carrier-based pulse-width modulation (PWM) strategy with zero-sequence components injection to suppress the voltage deviation of DC-link capacitors, but this method is very complex and not saving the calculation resource which is difficult to be applied in practice. In [9], a feed-forward method controlling neutral-point fluctuation using a fixed adjustment factor. However, the selection of the fixed adjustment factor depends on the engineering experience. More importantly, this method cannot solve the abnormal operating condition such as unbalanced load in a hybrid VIENNA rectifier.

The major contribution of this study is to present two neutral-point control methods with a hybrid algorithm and a simplified method based on zero-sequence component injection to suppress

the voltage deviation of DC-link capacitors in a hybrid-type VIENNA rectifier.

2. Methodology

2.1 Mathematical model of a hybrid VIENNA rectifier

The hybrid VIENNA topology is shown in Fig. 1 [10], which is composed of a diode bridge rectifier with a Boost unit and a VIENNA rectifier in parallel as shown in Fig. 2, each rectifier contributes parts of power, thus, the power and current stress in the switch of each rectifier would be reduced [11].

2.1.1 Reason analysing for neutral-point unbalance: The equation of DC-side two capacitors voltage and current can be analysed from the circuit shown in Fig. 2, which can be written as

$$\begin{cases} U_{C1} = \frac{1}{C_1} \int_0^t i_{c1} dt + U_{C10}, \\ U_{C2} = \frac{1}{C_2} \int_0^t i_{c2} dt + U_{C20}, \end{cases} \quad (1)$$

where U_{C10} and U_{C20} are the initial voltages of capacitor C_1 and capacitor C_2 , respectively.

From (1), the DC-link capacitors' voltage not only has an association with U_{C10} and U_{C20} but also related the real-time charge–discharging current to two capacitors. The neutral point current i_o contains a lot of alternating current fluctuations and DC offset components, which causes voltage deviation of DC-link capacitors. On the basis of analysing a large number of references about neutral-point fluctuation control in the three-level converter, the forms and reasons of neutral-point voltage unbalance can be categorised as shown in Fig. 3 [12–15].

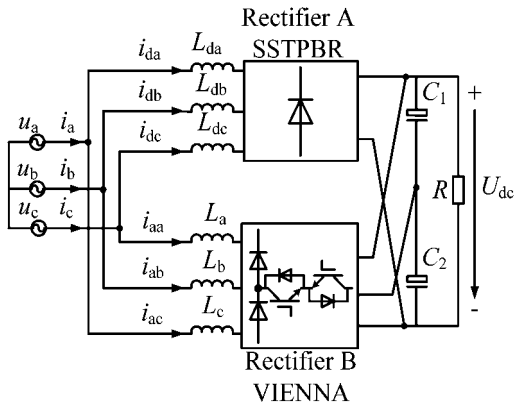


Fig. 1 Composition of hybrid VIENNA rectifier

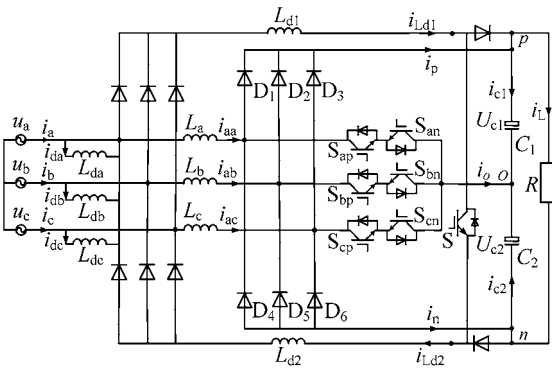


Fig. 2 Topology of hybrid VIENNA rectifier

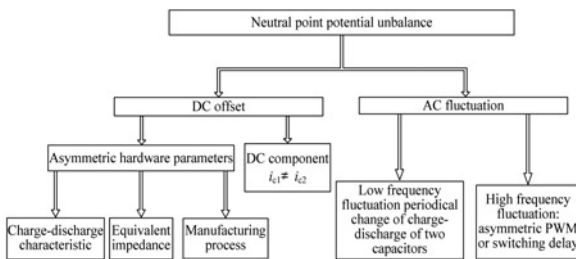


Fig. 3 Forms of neutral-point fluctuation

Seen from (1) and (2), the reason of voltage deviation of DC-link capacitors is that the value of current for charging and discharging between two capacitors are not equal.

Therefore, it is important to analyse the characteristics of charging and discharging feature between two DC-link capacitors by establishing a mathematical model of the neutral-point current i_o , so as to find an effective way to solve the problem of unbalance voltage of two DC-link capacitors in the hybrid VIENNA rectifier.

2.1.2 Neutral-point current mathematical model: As shown in Fig. 2, according to Kerchief's current law, the equations of the DC-side current can be written as follows:

$$\begin{pmatrix} i_p \\ i_n \end{pmatrix} = \begin{pmatrix} 1 \\ -1 \end{pmatrix} i_L + \begin{pmatrix} C_1 \frac{du_{c1}}{dt} - i_{Ld1} \\ C_2 \frac{du_{c2}}{dt} - i_{Ld2} \end{pmatrix}, \quad (2)$$

$$\begin{cases} i_o = -(i_{c1} + i_{c2}) = C_2 \frac{du_{c2}}{dt} - C_1 \frac{du_{c1}}{dt}, \\ i_o = \begin{pmatrix} S_a & & \\ & S_b & \\ & & S_c \end{pmatrix} \begin{pmatrix} i_a \\ i_b \\ i_c \end{pmatrix}. \end{cases} \quad (3)$$

S_i represents the switching states, which is shown in the following equation:

$$S_i = \begin{cases} 0 & S_i \text{ on.} \\ 1 & S_i \text{ off, } u_i > 0, i = a, b, c. \\ -1 & S_i \text{ off, } u_i < 0. \end{cases} \quad (4)$$

From (4), the important reason of voltage deviation of the DC-side capacitors is the neutral-point current whose value is not equal to zero. The charging and discharging of two capacitors lead to the neutral-point potential voltage fluctuation.

2.1.3 Low fundamental frequency mathematical model of neutral-point current: The value of capacitor C_1 is equal to capacitor C_2 in the ideal state; therefore, the neutral-point current expression is shown in the following equation:

$$\begin{cases} i_o = \left(\frac{du_{c2}}{dt} - \frac{du_{c1}}{dt} \right) C, \\ i_o = (1 - |u_{ta}|)i_a + (1 - |u_{tb}|)i_b + (1 - |u_{tc}|)i_c, \end{cases} \quad (5)$$

where u_{ta} , u_{tb} , and u_{tc} are the three-phase modulation signals, which are produced by closed loop control.

As shown in Fig. 4, the three-phase modulation signals can be divided into six sectors and each sector is 60° apart. Taking the sector 1 as an example, the three-phase modulation signals can be written as follows:

$$u_{ta} > 0, \quad u_{tb} > 0, \quad u_{tc} < 0. \quad (6)$$

Then, the neutral-point current can be expressed as follows:

$$i_o = u_{ta}i_a + u_{tb}i_b - u_{tc}i_c. \quad (7)$$

The sum of the three-phase modulation signals is zero for a normal three-phase system, which can be given by

$$u_{ta} + u_{tb} + u_{tc} = 0. \quad (8)$$

The three-phase current instantaneous value can be expressed by (9) when the hybrid rectifier is controlled by a closed-loop control system and has a unit power factor

$$i_i = k \cdot u_{ti}, \quad i = a, b, c, \quad (9)$$

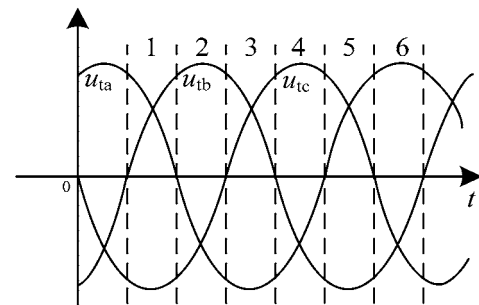


Fig. 4 Sector division of hybrid VIENNA rectifier

where k is the ratio index between the input current and the reference voltage.

With (7)–(9), the neutral-point fundamental frequency current can be expressed as follows:

$$i_0 = -2ku_{tb}u_{ta}. \quad (10)$$

The expressions of neutral-point current i_0 in the other five sectors can be calculated in the same way.

2.2 Hybrid adjustment factor control method to suppress voltage deviation of DC-link capacitors

From Fig. 2, the expression of voltage deviation of the DC-link capacitors is obtained as follows:

$$\Delta_{uc} = U_{C2} - U_{C1}. \quad (11)$$

Taking the sector 1 as an example, the expression of neutral-point current (shown in (8)) after being added to the voltage deviation of the DC-link capacitors can be written as follows:

$$\begin{aligned} \dot{i}_0 = & (1 + u_{ta} + m_t \Delta_{uc})i_a + (1 + u_{tb} + m_t \Delta_{uc})i_b \\ & + (1 - u_{tc} - m_t \Delta_{uc})i_c. \end{aligned} \quad (12)$$

Equations (7), (8), (10), and (12) can be simplified as

$$\dot{i}_0 = i_0 - 2m_t k u_{tc} \Delta_{uc}. \quad (13)$$

The neutral-point current (i_0) is added to the voltage deviation of DC-side capacitors (Δ_{uc}), whose amplitude is reduced and the neutral-point unbalanced would be eliminated.

The essential reason for the neutral-point voltage unbalanced is that the three-time fundamental frequency fluctuation of the neutral-point current is theoretically not equal to zero. Therefore, in order to solve this problem, (13) is equal to zero, combining (10), we have

$$m_t = -\frac{u_{tb}u_{ta}}{u_{tc}\Delta_{uc}}, \quad (14)$$

where m_t is the neutral-point hybrid adjustment factor. From (14), the value of the neutral-point adjustment factor is resolvable, which is expressed as follows:

$$u_{td} = m_t \Delta_{uc} = -\frac{u_{tb}u_{ta}}{u_{tc}}. \quad (15)$$

The expression of neutral-point adjustment factors in other sectors can be obtained in similar ways, which are shown in Table 1.

Equation (15) can suppress the neutral-point voltage deviation in theory. If the three-times fundamental frequency fluctuation of the neutral-point current is closed to nearly infinitesimal, the problem of the DC-link capacitors voltage deviation could be solved,

Table 1 Neutral-point adjustment factor and expressions

Sector	Neutral-point adjustment factor m_t	Neutral-point adjustment expression u_{td}
1, 4	$m_t = -\frac{u_{tb}u_{ta}}{u_{tc}\Delta_{uc}}$	$u_{td} = -\frac{u_{tb}u_{ta}}{u_{tc}}$
2, 5	$m_t = -\frac{u_{ta}u_{tc}}{u_{tb}\Delta_{uc}}$	$u_{td} = -\frac{u_{ta}u_{tc}}{u_{tb}}$
3, 6	$m_t = -\frac{u_{tb}u_{tc}}{u_{ta}\Delta_{uc}}$	$u_{td} = -\frac{u_{tb}u_{tc}}{u_{ta}}$

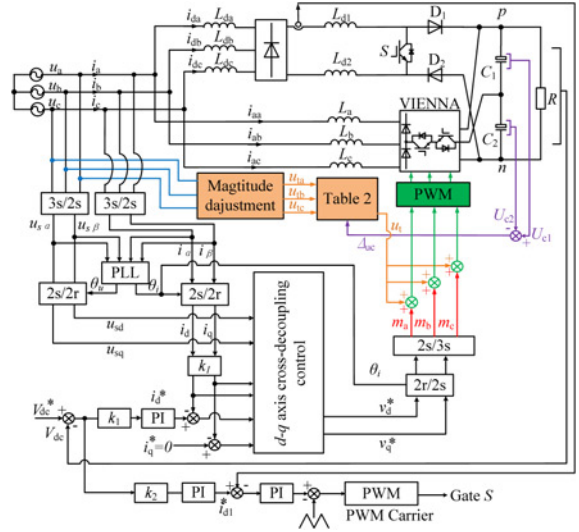


Fig. 5 Control system block diagram of d - q -axis cross-decoupling control based on the hybrid adjustment factor neutral-point control method

which means the value of the adjustment factor needs to be close to positive infinity, which can be expressed as follows:

$$\lim_{\Delta_{uc} \rightarrow 0} \left(m_t = -\frac{u_{tb}u_{ta}}{u_{tc}\Delta_{uc}} \right) = +\infty. \quad (16)$$

Fig. 5 shows a block diagram of d - q -axis cross-decoupling control based on the hybrid adjustment factor neutral-point control method. The component superimposed on the three-phase modulation waves (m_a, m_b, m_c) is u_t , which consists of two parts, the first part is the voltage deviation of DC-link capacitance Δ_{uc} , the second part is the adjustment factor calculated from Table 1, which is written as u_{td} . Then, the hybrid adjustment expression u_t can be expressed as follows:

$$u_t = u_{td} + \Delta_{uc}. \quad (17)$$

From (15) and (17), in the sector 1, u_t can be written as

$$u_t = \Delta_{uc} - \frac{u_{tb}u_{ta}}{u_{tc}} = \Delta_{uc} \left(1 - \frac{u_{tb}u_{ta}}{u_{tc}\Delta_{uc}} \right). \quad (18)$$

The hybrid adjustment factor expression in the other sectors can be calculated in the same way, which is shown in Table 2.

2.3 Simplified algorithm of neutral-point control based on zero – sequence component injection

The hybrid neutral-point control method can effectively control the voltage deviation of DC-link capacitors. However, this method needs complex computing resources. Therefore, it is necessary to

Table 2 Expressions of hybrid adjustment factors

Sector	The expression of hybrid adjustment factor $u_t = u_{td} + \Delta_{uc}$
1, 4	$u_t = \Delta_{uc} - \frac{u_{tb}u_{ta}}{u_{tc}}$
2, 5	$u_t = \Delta_{uc} - \frac{u_{ta}u_{tc}}{u_{tb}}$
3, 6	$u_t = \Delta_{uc} - \frac{u_{tb}u_{tc}}{u_{ta}}$

further simplify the neutral-point mathematical model; meanwhile, the neutral-point unbalance should also be controlled even under the abnormal condition such as unbalanced loads.

The three-phase modulation signals after being compensated with AC compensation of the neutral-point fluctuation d_i ($i = a, b, c$) can be divided into two parts

$$d_i = m_i + v_{ac}, \quad (19)$$

where m_i ($i = a, b, c$) is the three phase modulation signals of the hybrid VIENNA rectifier as shown in Fig. 5, v_{ac} is the AC compensation of the neutral-point fluctuation.

From (3) and (4), the neutral-point current i_o can be written as

$$-i_o = |d_a|i_a + |d_b|i_b + |d_c|i_c, \quad (20)$$

where the sign function can be defined as follows:

$$\text{sign}(x) = \begin{cases} 1 & x \geq 0, \\ 0 & x < 0. \end{cases} \quad (21)$$

In the closed-loop based on the classical d - q -axis cross-decoupling control system, due to the application of the phase-locked loop, the three-phase input voltages are in phase with the three-phase input current, therefore, the input voltages and currents with the same polarity. $|d_i|$ and i_i can be expressed as follows:

$$|d_i| = d_i(\text{sign}(i_i) + \text{sign}(-i_i)), \quad (22)$$

$$i_i = i_i(\text{sign}(i_i) + \text{sign}(-i_i)). \quad (23)$$

From (20), (22) and (23), the neutral-point current can be rewritten as

$$-i_o = d_a|i_a| + d_b|i_b| + d_c|i_c|. \quad (24)$$

To suppress DC-link capacitance voltage deviation, the neutral-point current i_o should always be zero within each sector. Therefore, from (20) and (24), the AC compensation of the neutral-point fluctuation can be given by

$$v_{ac} = -\frac{m_a|i_a| + m_b|i_b| + m_c|i_c|}{|i_a| + |i_b| + |i_c|}. \quad (25)$$

The zero sequence components consist of AC compensation of the neutral-point fluctuation v_{ac} and the voltage deviation of DC-link capacitors Δ_{uc} . Therefore, the zero sequence components (V_{com}) can be given by

$$V_{com} = v_{ac} + \Delta_{uc}. \quad (26)$$

A block diagram of the d - q -axis cross-decoupling control based on the simplified neutral-point control method for the hybrid VIENNA rectifier is shown in Fig. 6. The closed-loop control system is the classical d - q -axis cross-decoupling control which is the same as Fig. 5. The zero sequence component (V_{com}) combining an AC compensation of the neutral-point fluctuation and the voltage deviation of DC-link capacitors which are added to the three-phase modulation signals to solve the problem of the DC-link capacitors' voltage unbalanced for a hybrid rectifier.

2.4 Comparison between the two neutral-point control methods

The performance comparison of the neutral-point balance control between the two proposed control methods is shown in Table 3, the simplified algorithm of the neutral-point control method not only has the good performance in suppressing the voltage deviation of DC-link capacitors but also saving the computing resource of the digital signal processing (DSP) controller. In addition, the two

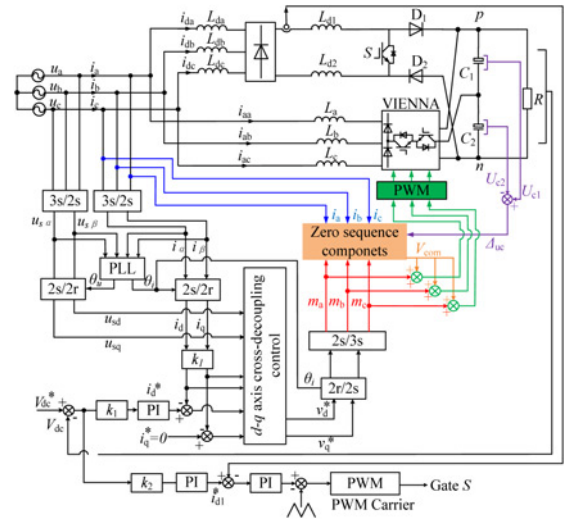


Fig. 6 Control system block diagram of d - q -axis cross-decoupling control based on the simplified neutral-point control method

Table 3 Comparison between the two neutral-point control methods

Performance	Control method	
	Hybrid neutral-point control method	The simplified algorithm of the neutral-point method
input current THD	reduced	further reduced
fundamental frequency component three times	reduced	further reduced
fundamental frequency component		
computing resources of the control method	more	little

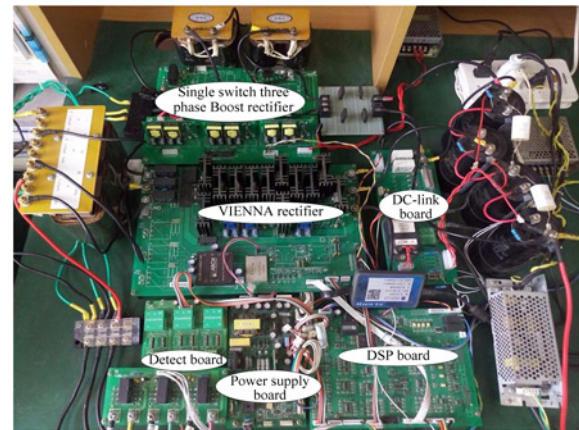


Fig. 7 Experimental prototype

control methods can suppress the three times fundamental frequency component of neutral-point current, which is the reason for the DC-link capacitors' voltage unbalanced in the hybrid VIENNA rectifier (Fig. 7).

3 Results

To verify the feasibility of the two control methods shown in Figs. 5 and 6, respectively, a power experiment platform was built

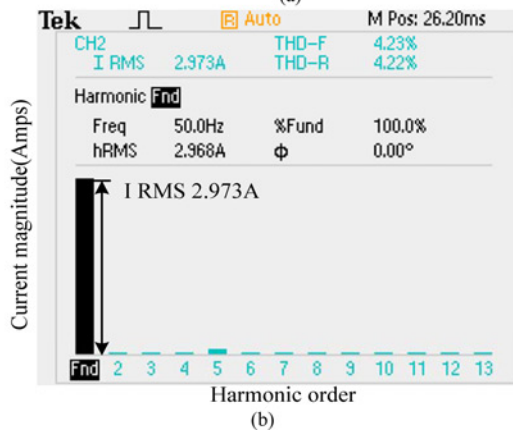
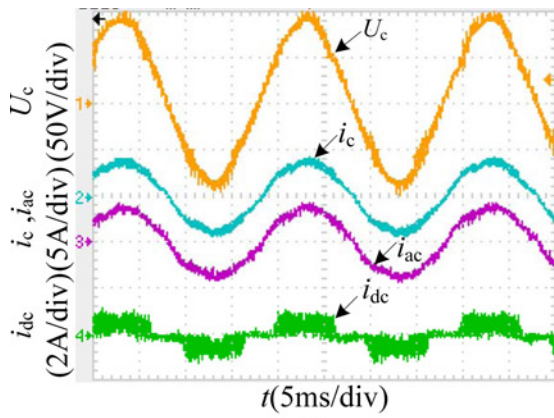


Fig. 8 Input voltage, input current and harmonic order of the hybrid VIENNA rectifier without neutral-point balancing control
a Input voltage and input current of hybrid VIENNA rectifier, input current of VIENNA rectifier and input current of Boost rectifier
b Harmonic order of input phase current of hybrid VIENNA rectifier

controlled by a 32-bit DSP-type TMS320F2812, which is shown in Fig. 8, and the experimental parameters are shown in Table 4.

Figs. 8a and b show the input voltage, input phase current of the hybrid VIENNA rectifier (i_c), input phase current of VIENNA rectifier (rectifier A) (i_{ac}), input phase current of a single-switch three-phase Boost rectifier (rectifier B) (i_{dc}), and the fundamental harmonic of input current (i_c) without the proposed neutral-point balancing control methods in a hybrid VIENNA rectifier. It can be seen that Boost rectifier takes a part of the input current of this hybrid rectifier as well as reduces the current stress of the VIENNA rectifier. The THD of input current (i_c) is 4.23%, which is also lower than THD = 5%, which illustrates that the hybrid VIENNA rectifier has a good performance in low THD and PF under the $d-q$ -axis cross-decoupling control system.

Fig. 9 shows the waveforms of input phase current (i_c), the voltage of two DC-link capacitors (U_{c1} , U_{c2}) and capacitors voltage deviation ($U_{c1}-U_{c2}$) without neutral-point control method. In Fig. 9a, the voltage of DC-link capacitors is measured with a DC coupling channel, it can be seen that voltage deviation of two

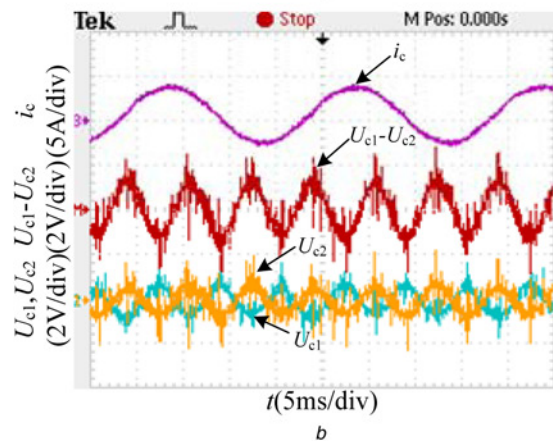
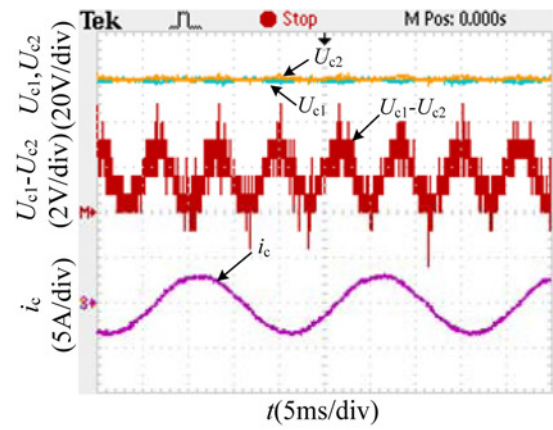


Fig. 9 Waveforms without neutral-point control method

DC-link capacitors ($U_{c1}-U_{c2}$) is up to 5 V. In Fig. 9b, the voltage of DC-link capacitors is measured with an AC coupling channel, it can be seen that the voltage deviation of three-time fundamental frequency fluctuation is up to ± 3 V, which is not equal to 0 V. Therefore, the neutral-point potential fluctuation in the VIENNA three-level rectifier is also reflected in the hybrid VIENNA rectifier.

Fig. 10 shows the waveforms of input phase current (i_c), the voltage of two DC-link capacitors (U_{c1} , U_{c2}) and capacitors voltage deviation ($U_{c1}-U_{c2}$) with the hybrid adjustment factor control method and the proposed simplified algorithm of the neutral-point method. In Figs. 10a and c, t voltage of two DC-link capacitors (U_{c1} , U_{c2}) is measured with a DC coupling channel, which can be seen that the voltage deviation of two DC-link capacitors ($U_{c1}-U_{c2}$) is up to 3.2 V, which is not effectively suppressed when using the hybrid adjustment factor control method, but by applying the simplified algorithm of neutral-point control, the neutral-point voltage deviation ($U_{c1}-U_{c2}$) is reduced within 2.4 V, which has been effectively reduced. In Figs. 10b and d, the voltage of DC-link capacitors is measured with an AC coupling channel, which can be seen that the voltage deviation of three-time fundamental frequency component ($U_{c1}-U_{c2}$) is up to ± 1.6 V when using the hybrid adjustment factor control method, and by using the simplified algorithm of neutral-point control, it is reduced to within ± 1 V, which verifies the validity of the proposed two control methods.

Fig. 12 shows the effect comparison waves of different neutral-point control method under the unbalanced loads conditions ($C_1:1100 \mu\text{F}$, $C_2:1650 \mu\text{F}$, $R_1:40 \Omega$, $R_2:50 \Omega$). The equivalent circuit of abnormal load condition is shown in Fig. 11. From waves, it can be seen that the voltage deviation ($U_{c1}-U_{c2}$) is effectively suppressed when using the proposed two neutral-point balancing control methods compared with no neutral-point balancing

Table 4 Experimental parameters

grid-voltage	100 V/50 Hz
DC-link voltage reference	200 V
load resistor	90 Ω
AC-filter inductor of VIENNA	10 mH
DC-inductor of BOOST	2.5 mH
DC-link filter capacitor	3300 μF
switching frequency	10 kHz

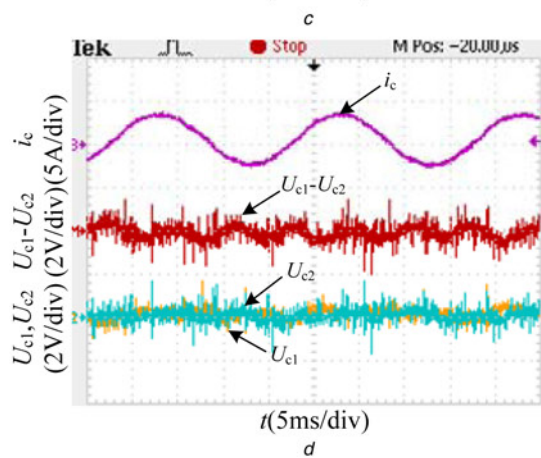
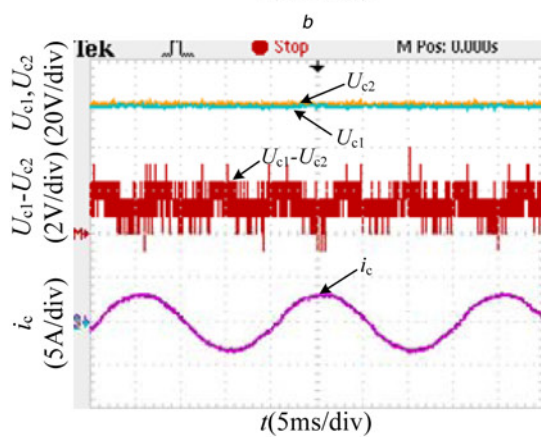
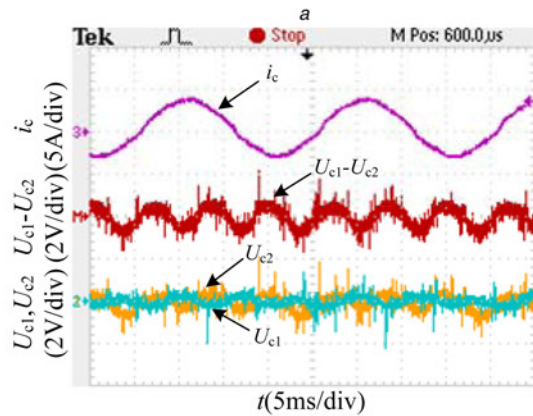
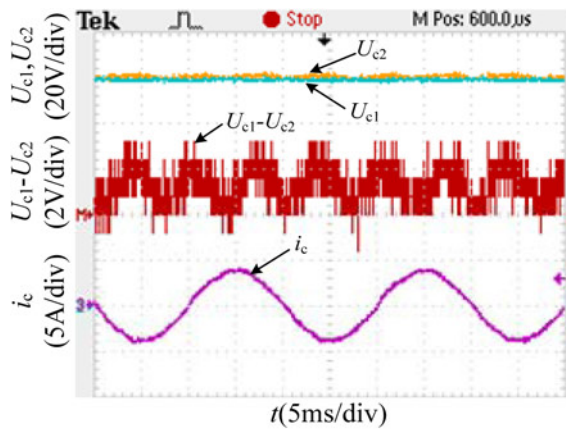


Fig. 10 Comparison waveforms between (a), (b) Proposed hybrid method, (c), (d) Proposed simplified algorithm of neutral-point control method

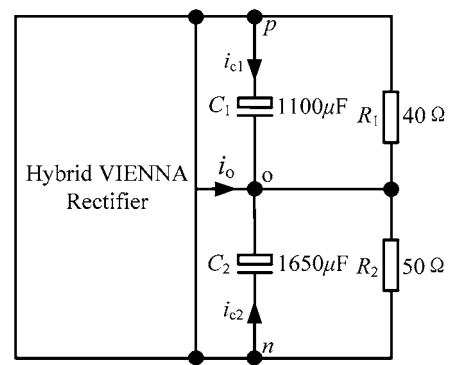


Fig. 11 The equivalent circuit of unbalanced load

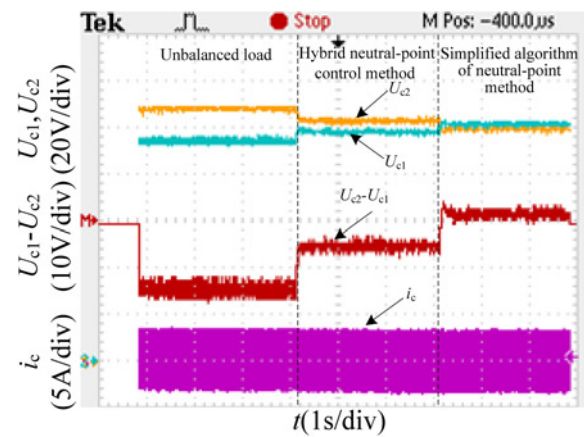


Fig. 12 The effect comparison waves of different neutral-point balancing control method under unbalanced loads condition

control. Furthermore, by applying the simplified algorithm of the neutral-point control method, the voltage deviation ($U_{c1}-U_{c2}$) is further suppressed, and the neutral-point voltage fluctuation has been effectively reduced, which verify the validity of the proposed simplified algorithm of the neutral-point control method can be applied under the abnormal operating condition such as unbalanced load.

4 Conclusion

This study presents two control methods to solve the problem of the voltage deviation of DC-link capacitors in a hybrid rectifier consisted of a three-level VIENNA rectifier and a three-phase diode bridge boost-type rectifier. The voltage deviation of DC-link capacitors can be effectively reduced as well as a three-time fundamental frequency component of neutral-point current can be eliminated under the two proposed control methods. The hybrid adjustment control method needs to divide the three-phase modulation signals into six sectors, and then find the corresponding adjustment factor in each sector to suppress the voltage deviation. The simplified algorithm of the neutral-point control method further simplifies the computing resources and has a better control effect on suppressing voltage deviation of DC-link capacitors even under the abnormal conditions such as unbalanced loads, which is suitable for practical implementation and broadens the engineering application of the hybrid VIENNA rectifier.

5 Acknowledgments

This project was supported by the National Natural Science Foundation of China (51307138), the Shaanxi International Exchange and Cooperation Project (2017KW-035), the State Key Laboratory of Large Electric Drive System and Equipment

6 References

- [1] Izadinia A., Karshenas H.: 'Current shaping in a hybrid 12-pulse rectifier using Vienna rectifier', *IEEE Trans. Power Electron.*, 2017, **33**, (2), pp. 1135–1142
- [2] Lima G.B., Finazzi A.P., Freitas L.C., *ET AL.*: 'Single-phase high power factor hybrid rectifier suitable for high-power applications', *IET Power Electron.*, 2012, **5**, (7), pp. 1137–1146
- [3] Costa A.V., Rodrigues D.B., Lima G.B., *ET AL.*: 'New hybrid high-power rectifier with reduced THDI and voltage-sag ride-through capability using boost converter', *IEEE Trans. Ind. Appl.*, 2013, **49**, (6), pp. 2421–2436
- [4] Soeiro T.B., Friedli T., Hartmann M., *ET AL.*: 'New unidirectional hybrid delta-switch rectifier'. Proc. IECON 37th Annual Conf. of the IEEE Industrial Electronics Society, Melbourne, Australia, November 2011, pp. 1474–1479
- [5] Wu H.: 'Interleaved LLC resonant converter with hybrid rectifier and variable-frequency plus phase-shift (VFPPS) control for wide output voltage range applications', *IEEE Trans. Power Electron.*, 2016, **32**, (6), pp. 4246–4257
- [6] Soeiro T.B., Kolar J.W.: 'Analysis of high-efficiency three-phase two- and three-level unidirectional hybrid rectifiers', *IEEE Trans. Ind. Electron.*, 2012, **60**, (9), pp. 3589–3610
- [7] Thangavelu T., Shanmugam P., Raj K.: 'Modelling and control of VIENNA rectifier a single phase approach', *IET Power Electron.*, 2015, **8**, (12), pp. 2471–2482
- [8] Wang Z., Cui F., Zhang G., *ET AL.*: 'Novel carrier-based PWM strategy with zero-sequence voltage injected for three-level NPC inverter', *IEEE J. Emerging Sel. Top. Power Electron.*, 2016, **4**, (4), pp. 1442–1451
- [9] Song W., Huang J., Zhong Y.: 'Hysteresis current control method of VIENNA rectifier with midpoint potential balance control', *Power Syst. Technol.*, 2013, **37**, (7), pp. 1909–1914 (in Chinese)
- [10] Alves R.L., Font C.H.L., Barbi I.: 'A novel unidirectional hybrid three-phase rectifier system employing boost topology'. Proc. 2005 IEEE 36th Power Electronics Specialists Conf., Recife, Brazil, June 2005, pp. 487–493
- [11] Alves R.L., Barbi I.: 'Analysis and implementation of a hybrid high-power-factor three-phase unidirectional rectifier', *IEEE Trans. Power Electron.*, 2009, **24**, (3), pp. 632–640
- [12] Zhang M., Hang L., Yao W., *ET AL.*: 'A novel strategy for three-phase/switch/level (Vienna) rectifier under severe unbalanced grids', *IEEE Trans. Ind. Electron.*, 2013, **60**, (10), pp. 4243–4252
- [13] Hang L., Li B., Zhang M., *ET AL.*: 'Equivalence of SVM and carrier-based PWM in three-phase/wire/level Vienna rectifier and capability of unbalanced-load control', *IEEE Trans. Ind. Electron.*, 2014, **61**, (1), pp. 20–28
- [14] Zhao W., Ruan X., Yang D., *ET AL.*: 'Neutral point voltage ripple suppression for three-phase four-wire inverter with independently-controlled neutral module', *IEEE Trans. Ind. Electron.*, 2017, **64**, (4), pp. 2608–2619
- [15] Narendrababu, Agarwal P.: 'A hybrid modulation strategy for eliminating low frequency NP voltage oscillations in NPC using redistribution of NTV duty ratios', *IET Power Electron.*, 2017, **10**, (12), pp. 1504–1517